Wave Motion 49 (2012) 347–363

Contents lists available at SciVerse ScienceDirect

Wave Motion

journal homepage: www.elsevier.com/locate/wavemoti

The Riemann–Volterra time-domain technique for waveguides: A case study for elliptic geometry

Andrei B. Utkin *

INOV - Inesc Inovação, Rua Alves Redol 9, Lisbon 1000-029, Portugal
ICEMS, Instituto Superior Técnico, Technical University of Lisbon, Av. Rovisco Pais 1, Lisbon 1049-001, Portugal

ARTICLE INFO

Article history:
Received 17 June 2011
Received in revised form 14 November 2011
Accepted 1 December 2011
Available online 8 December 2011

Keywords:
Wave equation
Mathieu function
Waveguide
Incomplete separation of variables

ABSTRACT

The method of incomplete separation of variables is applied for solving the wave propagation problems in which the source distribution and the emanated wave are constrained by an elliptic cylinder. Solutions are obtained in the form of expansions in terms of the Mathieu modes, whose completeness makes possible to solve the problem for arbitrary source distribution and initial values of the wavefunction and its time derivative defined within the cylinder. Transient modal amplitudes are found using the Riemann (Riemann–Volterra) method. An important feature of this approach is the straightforward definition of the essentially bounded effective integration areas on the plane spanned by the longitudinal and time coordinates, taking into account the spatiotemporal constraints imposed on the source. For source turned on in a fixed instant, the method is capable to model wave propagation inside the semi-infinite and finite elliptic cylinders provided that the Dirichlet or Neumann boundary conditions are specified on the limiting cross-section(s). Recent techniques of transverse–longitudinal wave decomposition open the prospect of adapting the method to more general cylindrical configurations and to other cases, in which the incomplete separation of variables results in partial differential equations of a known Riemann function (such as the Euler–Poisson–Darboux equation).

1. Introduction

Theoretical studies of wave phenomena usually imply separation of variables in the descriptive equations by a suitable integral transform or series expansion in terms of eigenfunctions (modes). In the time-domain methods, the temporal and one of the spatial variables remain unseparated, resulting in a hyperbolic-type partial differential equation (PDE). In the (general type) cylindrical coordinates, composing spacetime u, v, z, τ (where z is a Cartesian coordinate and $\tau = ct$ is the time variable in units of length, c being the wavefront velocity) the above PDE is the Klein–Gordon equation (KGE). The solving schemes for the electromagnetic problems include three stages: scalarization of Maxwell's equations, separation of the transverse coordinates u, v, and solving the resulting Klein–Gordon problem.

Some prospective modern time-domain methods — e.g., the modal decomposition via a wave splitting technique — described in [1–5] and references therein, provide solutions for a wide range of problems, including the general case of a cylindrical waveguide or cavity of any reasonable cross-section (see [6] for strict mathematical discussion). At solving the derived problems, the overwhelming majority of studies rely upon representation of the desired solution as a time convolution of a corresponding Green function with the source term. Another approach encompasses Miller's variable substitution [7] and using the symmetry of the KGE under the action of the Poincare group for solution factorization [5]. One

* Correspondence to: ICEMS, Instituto Superior Técnico, Technical University of Lisbon, Av. Rovisco Pais 1, Lisbon 1049-001, Portugal. Tel.: +351 213100426; fax: +351 213100445.
E-mail address: andrei.utkin@inov.pt.

0165-2125/$ – see front matter
doi:10.1016/j.wavemoti.2011.12.001

more technique less discussed in the literature is based on the Riemann–Volterra method. It permits constructing solutions to the wave problems in the case of both the inhomogeneous initial conditions and source term within the framework of unique formula. The method was successfully applied to a number of scalar and electromagnetic wave problems, including the spherical harmonic expansion of the fields produced by transient sources in free space [8] and dispersive media [9], electromagnetic fields generated by line current pulses [10], as well as wave propagation in planar, rectangular and circular waveguides and conical horns [11].

The present research significantly extends the application the Riemann–Volterra method for the description of wave propagation in the general-type cylindrical waveguides, enabling one to construct solutions to a wide range of the inhomogeneous problems not only for the infinite-waveguide models ($-\infty < z < \infty$), but for the semi-infinite ($0 < z < \infty$) and finite ($0 < z < L = const$) cylindrical structures as well, provided that either the Dirichlet or Neumann boundary condition is imposed at each limiting cross-section.

Despite the general nature of the developed Riemann–Volterra procedure, the derivation of the KGE is carried out and some illustrative numerical results are shown for a particular case of the elliptic cylinder, for which the natural choice of the transverse variables u, v is $x = h\cosh u\cos v$, $y = h\sinh u\sin v$, where x and y represent the Cartesian coordinates and h is the semifocal length of the fundamental ellipse. Such a case study is interesting for the following reasons: (i) The market of elliptical waveguides demonstrated a tremendous growth. During the last two decades, a considerable amount of knowledge has been accumulated, demonstrating several advantages of the elliptical-cross-section waveguides and fibers over those of the circular cross-section [12,13]. Modern computer-controlled fabrication tools resolved the problems of manufacturing elliptical shapes and stimulated further extensive research in the field in question, a state-of-the-art example is discussed in [13,14]. (ii) Constructing solution in the elliptic cylinder coordinates stays apart from similar schemes for the Cartesian, circular cylinder, and spherical coordinates, demonstrating a case of mutual inseparability of the transverse variables: the wavefunction can only be taken in the form $\Psi(u, v, z, \tau) = \psi_\perp(u, v)\,\psi_\parallel(z, \tau)$, with no way to reduce it to $\Psi(u, v, z, \tau) = \psi_1(u)\,\psi_2(v)\,\psi_\parallel(z, \tau)$ or introduce a convenient integral transform. (iii) The result provides a fresh illustration of reduction of the inhomogeneous wave problem to the inhomogeneous KG problem. As will be shown, the completeness of the involved Mathieu modes, scarcely discussed in the literature, makes it possible to obtain the modal expansion for arbitrary source term and initial conditions imposed on the wavefunction and its time derivative.

The potentials of the general modal solution derived in Section 2 are examined in Section 3 for the source turned on at a fixed moment of time. In particular, the symmetry of the modal solution and the adaption of the general formulas to the cases of semi-infinite and finite configurations (waveguides and cavities) are discussed. The versatility of the developed technique is further illustrated in Sections 4 and 5 for practically important cases of finite-length, finite-duration sources, quiescent and traveling, by deriving *ad hoc* integral formulas and presenting numerical results.

2. General modal solution

2.1. Initial-boundary value problem

A variety of problems describing the wave propagation within an elliptic cylinder can be reduced to one or several scalar initial-boundary value problems of the type

$$\Box\Psi(u, v, z, \tau) = \left[\partial_\tau^2 - \frac{1}{h^2\left(\cosh^2 u - \cos^2 v\right)}\left(\partial_u^2 + \partial_v^2\right) - \partial_z^2\right]\Psi(u, v, z, \tau) = S(u, v, z, \tau), \tag{1}$$

$$\Psi|_{\tau=0} = \psi(u, v, z), \qquad \partial_\tau\Psi|_{\tau=0} = \hat{\psi}(u, v, z), \tag{2}$$

where the wavefunction Ψ stands for some potential or its derivative and S for the source term. Additionally, we will suppose that the potential function is chosen in such a way that it nulls at the elliptic boundary of the cylinder cross-section $u = u_0 = const$; in particular, it corresponds to the model of perfectly conducting walls (see, for example, [13] and [15, Chapter 18]). As a consequence, there is no field outside the cylinder, and one can write

$$\Psi(u, v, z, \tau) = 0, \qquad \psi(u, v, z) = 0, \qquad \hat{\psi}(u, v, z) = 0, \qquad S(u, v, z, \tau) = 0 \quad \text{for } u > u_0. \tag{3}$$

We will find the unique solution of this general initial-boundary value problem for the arbitrary functions S, ψ, and $\hat{\psi}$, integrable within the elliptic domain $\mathcal{E}_{uv} = \{0 \le u \le u_0, 0 \le v < 2\pi\}$.

2.2. Statement of the modal amplitude problem

For arbitrary S, ψ, and $\hat{\psi}$, the possibility of deriving the KGE from the wave equation (1) is provided by completeness of the Mathieu sine and cosine modes, proved by Goldstein [16], which enables us to write (for the domain of interest $\mathcal{E}_{uv}$)

the expansions similar to that describing the steady-state vibrational modes of a stretched membrane having an elliptical boundary [15, Section 16.14]

$$\begin{pmatrix}\psi\,(u,v,z)\\ \hat{\psi}\,(u,v,z)\\ S\,(u,v,z,\tau)\end{pmatrix}=\sum_{m=0}^{\infty}\sum_{n=1}^{\infty}\begin{pmatrix}\psi_{mn}^{(e)}(z)\\ \hat{\psi}_{mn}^{(e)}(z)\\ S_{mn}^{(e)}(z,\tau)\end{pmatrix}\mathrm{Ce}_m\left(u,q_{mn}^{(e)}\right)\mathrm{ce}_m\left(v,q_{mn}^{(e)}\right)$$
$$+\sum_{m=1}^{\infty}\sum_{n=1}^{\infty}\begin{pmatrix}\psi_{mn}^{(o)}(z)\\ \hat{\psi}_{mn}^{(o)}(z)\\ S_{mn}^{(o)}(z,\tau)\end{pmatrix}\mathrm{Se}_m\left(u,q_{mn}^{(o)}\right)\mathrm{se}_m\left(v,q_{mn}^{(o)}\right), \tag{4}$$

where $\mathrm{ce}_m(v,q)$ and $\mathrm{se}_m(v,q)$ stand for the Mathieu cosines and sines; $\mathrm{Ce}_m(u,q)=\mathrm{ce}_m(iu,q)$, $\mathrm{Se}_m(u,q)=-i\,\mathrm{se}_m(iu,q)$ are the radial Mathieu functions of the first kind of order m; the constants $q_{mn}^{(e)}$, $q_{mn}^{(o)}$ are the n-th roots of these functions, $\mathrm{Ce}_m\left(u_0,q_{mn}^{(e)}\right)=0$, $\mathrm{Se}_m\left(u_0,q_{mn}^{(o)}\right)=0$; and $\psi_{mn}^{(e,o)}$, $\hat{\psi}_{mn}^{(e,o)}$, $S_{mn}^{(e,o)}$ are known functions derived from ψ, $\hat{\psi}$, S using the orthogonality properties of the Mathieu modes as demonstrated in Appendix A.

Seeking the desired wavefunction $\Psi(u,v,z,\tau)$ in the form of the same modal expansion

$$\Psi(u,v,z,\tau)=\sum_{m=0}^{\infty}\sum_{n=1}^{\infty}\Psi_{mn}^{(e)}(z,\tau)\,\mathrm{Ce}_m\left(u,q_{mn}^{(e)}\right)\mathrm{ce}_m\left(v,q_{mn}^{(e)}\right)+\sum_{m=1}^{\infty}\sum_{n=1}^{\infty}\Psi_{mn}^{(o)}(z,\tau)\,\mathrm{Se}_m\left(u,q_{mn}^{(o)}\right)\mathrm{se}_m\left(v,q_{mn}^{(o)}\right), \tag{5}$$

and substituting (4), (5) into (1) and (2) yield the problem for the modal amplitudes $\Psi_{mn}^{(e,o)}(z,\tau)$

$$\left[\partial_\tau^2-\partial_z^2+\left(k_{mn}^{(e,o)}\right)^2\right]\Psi_{mn}^{(e,o)}(z,\tau)=S_{mn}^{(e,o)}(z,\tau),\qquad k_{mn}^{(e,o)}=\frac{2\sqrt{q_{mn}^{(e,o)}}}{h},$$
$$\Psi_{mn}^{(e,o)}\big|_{\tau=0}=\psi_{mn}^{(e,o)}(z),\qquad \partial_\tau\Psi_{mn}^{(e,o)}\big|_{\tau=0}=\hat{\psi}_{mn}^{(e,o)}(z). \tag{6}$$

2.3. Exact solution for the modal amplitude

Applying the linear coordinate transformation $\tau=X+Y$, $z=X-Y$ one converts problem (6) into

$$\left(\partial_{XY}^2+k^2\right)\Phi(X,Y)=\sigma(X,Y),$$
$$\Phi(X,Y)|_{X+Y=0}=\psi(X-Y),\qquad \left[\frac{1}{2}\left(\partial_X+\partial_Y\right)\Phi(X,Y)\right]\Big|_{X+Y=0}=\hat{\psi}(X-Y), \tag{7}$$

where $\Phi(X,Y)\overset{def}{=}\Psi(X+Y,X-Y)$ and $\sigma(X,Y)\overset{def}{=}S(X+Y,X-Y)$ (throughout this subsection, the indices o, e, m and n are dropped for simplicity of notation). Solving problem (7) reduces to definition of the function Φ at an arbitrary point X_0, Y_0 of the X, Y plane, provided that the initial data for Φ and its normal derivative are given on the line AB, $X+Y=0$, as shown in Fig. 1. This can be done using the Riemann–Volterra method (see, for example, [17]):

$$\Phi(X_0,Y_0)=\frac{1}{2}\left[(R\Phi)|_{\substack{X=X_A\\Y=Y_A}}+(R\Phi)|_{\substack{X=X_B\\Y=Y_B}}\right]$$
$$+\int_{AB}\left[dX\left(\frac{1}{2}R\,\partial_X\Phi-\frac{1}{2}\Phi\,\partial_X R\right)-dY\left(\frac{1}{2}R\,\partial_Y\Phi-\frac{1}{2}\Phi\,\partial_Y R\right)\right]+\iint_\Omega dXdY\,R\sigma, \tag{8}$$

where $R(X,Y;X_0,Y_0)=J_0\left(\sqrt{4k^2(X-X_0)(Y-Y_0)}\right)$ is the Riemann function for the first canonical form of the KGE (7) and J_0 the Bessel function of the first kind of order zero. Noticing that $\Phi|_{\substack{X=X_A\\Y=Y_A}}=\psi(X_A-Y_A)$, $\Phi|_{\substack{X=X_B\\Y=Y_B}}=\psi(X_B-Y_B)$, $X_A=-Y_0$, $Y_A=Y_0$, $X_B=X_0$, $Y_B=-X_0$, as well as $dY=-dX$ and $\frac{1}{2}(\partial_X+\partial_Y)\Phi=\hat{\psi}(X-Y)$ on AB, formula (8) can be reduced to

$$\Phi(X_0,Y_0)=\frac{1}{2}\left[R|_{\substack{X=X_A\\Y=Y_A}}\psi(-2Y_0)+R|_{\substack{X=X_B\\Y=Y_B}}\psi(2X_0)\right]$$
$$+\int_{-Y_0}^{X_0}dX\left[R\hat{\psi}(X-Y)-\psi(X-Y)\frac{1}{2}\left(\partial_X+\partial_Y\right)R\right]\Big|_{Y=-X}+\iint_\Omega dXdYR\sigma. \tag{9}$$

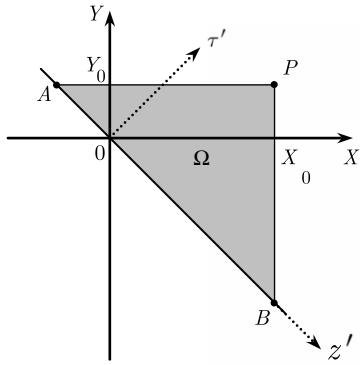

Fig. 1. An X, Y plane diagram for definition of the modal amplitude at the point $P(X0, Y0)$.

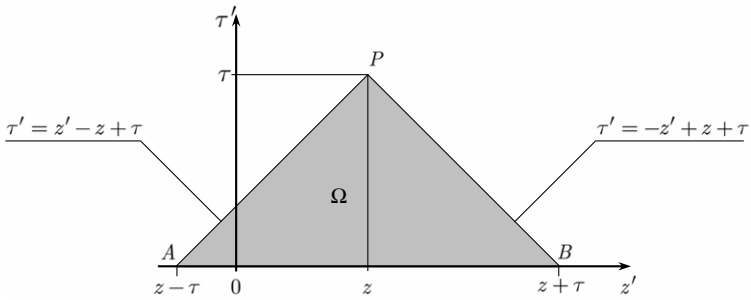

Fig. 2. A z', τ' plane diagram for definition of the modal amplitude at the point $P(z, \tau)$.

2.4. General modal solution in the space-time domain

Coming back to the initial coordinate system by the substitution $X_0 = \frac{1}{2}(\tau + z)$, $Y_0 = \frac{1}{2}(\tau - z)$, $X = \frac{1}{2}(\tau' + z')$, $Y = \frac{1}{2}(\tau' - z')$, so that $dXdY = \frac{\partial(X,Y)}{\partial(\tau',z')} d\tau' dz' = \frac{1}{2} d\tau' dz'$ and $X = \frac{1}{2}z'$, $Y = -\frac{1}{2}z'$ on AB, we finally construct the desired solution to problem (6)

$$\begin{aligned}\Psi_{mn}^{(e,o)}(z,\tau) = {} & \frac{1}{2}\left[R(z-\tau,0;z,\tau)\,\psi_{mn}^{(e,o)}(z-\tau) + R(z+\tau,0;z,\tau)\,\psi_{mn}^{(e,o)}(z+\tau)\right] \\ & + \frac{1}{2}\int_{z-\tau}^{z+\tau} dz' \left[R(z',0;z,\tau)\,\hat{\psi}_{mn}^{(e,o)}(z') - \partial_{\tau'} R(z',0;z,\tau)\,\psi_{mn}^{(e,o)}(z')\right] \\ & + \frac{1}{2}\iint_{\Omega} dz' d\tau' R(z',\tau';z,\tau)\,S_{mn}^{(e,o)}(z',\tau'),\end{aligned} \tag{10}$$

where

$$R(z',\tau';z,\tau) = J_0\left(k_{mn}^{(e,o)}\sqrt{(\tau'-\tau)^2 - (z'-z)^2}\right) \tag{11}$$

stands for representation of the Riemann function in the z', τ' domain, and the integration area Ω corresponds to the 45° right triangle shown in Fig. 2. The general-type modal solution to the original problem (1)–(3) is expansion (5) in which the modal amplitudes $\Psi_{mn}^{(e,o)}$ are represented by Eq. (10).

The Riemann–Volterra method is used in particular for proving the fact that the solution provided by integral formula (8) or (10) is unique [18]. The modal amplitude (10) represents an alternative to the classical Green function solution and, as one might expect, in the particular case of zero initial conditions coincides with the convolution of a causal Green function and the source term (cf. solution (16), (20) constructed by Geyi in [3]). An important feature of the Riemann–Volterra ansatz is the straightforward introduction of the restricted integration area on the z', τ' plane, an idea that may be further exploited for deriving explicit formulas for waves emanated by sources constrained in space-time (as all the real-world sources are). As the huge variety of practically interesting particular restrictions and features of the sources cannot be covered by universal formulas, the subsequent sections will be devoted to introduction of some sufficiently general procedures allowing to describe the wave propagation in the domains that are semi-infinite or finite in the longitudinal direction.

3. Source turned on at a fixed instant

3.1. Source turned on at a fixed instant: modal solution and its symmetry

A wave source turned on at a fixed instant, taken as $\tau = 0$, does not generate waves prior to this instant, which results in problem (1)–(3) with

$$S(u, v, z, \tau) \equiv 0 \qquad \Rightarrow \qquad \Psi(u, v, z, \tau) \equiv 0,\ \partial_\tau \Psi(u, v, z, \tau) \equiv 0 \quad \text{for } \tau < 0, \tag{12}$$

having a simpler modal solution

$$\begin{aligned} \Psi_{mn}^{(e,o)}(z, \tau) &= \frac{1}{2} \iint_{\Omega} dz' d\tau' J_0\left(k_{mn}^{(e,o)} \sqrt{(\tau' - \tau)^2 - (z' - z)^2}\right) S_{mn}^{(e,o)}(z', \tau') \\ &= \int_0^{\tau} d\tau' \mathcal{F}_{mn}^{(e,o)}(\tau', z, \tau), \end{aligned} \tag{13}$$

where

$$\mathcal{F}(\tau', z, \tau) \stackrel{def}{=} \frac{1}{2} \int_{z-(\tau-\tau')}^{z+(\tau-\tau')} dz' R_0(z' - z, \tau' - \tau) S(z', \tau'), \qquad R_0(z, \tau) \stackrel{def}{=} J_0\left(k\sqrt{\tau^2 - z^2}\right) \tag{14}$$

(throughout the remainder of this subsection we again suppress the superscripts and subscripts in $\Psi_{mn}^{(e,o)}$, $k_{mn}^{(e,o)}$, $S_{mn}^{(e,o)}$ and $\mathcal{F}_{mn}^{(e,o)}$, as they play no role in the subsequent analysis).

The calculation of the modal amplitude $\Psi(z, \tau)$ involves integration of the product $R_0(z' - z, \tau' - \tau) S(z', \tau')$ over a segment of the z' axis that unrestrictedly expands with increase of the observation time τ and thus requires definition of the source term $S(z, \tau)$ for all values of z. As a consequence, formulas (13), (14) can only be applied to the infinite model configurations ($-\infty < z < \infty$). Is it possible to extend the results to the semi-infinite ($0 < z < \infty$) and finite ($0 < z < L = const$) waveguiding systems? Previous investigations carried out for the problems conforming the spherical geometry (r, ϕ, θ) [8,9,11], possessing the natural restriction $r > 0$, indicate such a possibility, at least for the case of the Dirichlet condition imposed at $r = 0$: for the resulting Euler–Poisson–Darboux equation, the Riemann–Volterra solution was constructed by reconfiguring the initially triangle domain of integration over r', τ' into a trapezium that always lies in the region $r' > 0$ (see, e.g., Fig. 1(b) of [8]). This reconfiguration relies on the specific symmetry property of the Riemann function, which is either odd or even with respect to r'. As seen from Eq. (11), the Riemann function of the KGE does not possess the same property with respect to z', and here we must explore other symmetries for the desired extension of the method applicability.

With the help of Leibniz's theorem (see, e.g., Subsection 1.5(iv) of [19]), solution (13) gives the quadrature formulas for modes of the potential derivatives, which are directly connected with the field components. In particular, the z component of the potential gradient is

$$\partial_z \Psi(z, \tau) = \int_0^{\tau} d\tau' \partial_z \mathcal{F}(\tau', z, \tau), \tag{15}$$

where

$$\begin{aligned} \partial_z \mathcal{F}(\tau', z, \tau) &= \frac{S(z + (\tau - \tau'), \tau') - S(z - (\tau - \tau'), \tau')}{2} \\ &\quad - \frac{k}{2} \int_{z-(\tau-\tau')}^{z+(\tau-\tau')} dz' (z' - z) R_1(z' - z, \tau' - \tau) S(z', \tau'), \\ R_1(z, \tau) &\stackrel{def}{=} J_1\left(k\sqrt{\tau^2 - z^2}\right) / \sqrt{\tau^2 - z^2}. \end{aligned}$$

Changing the variable of integration to $\varsigma = |z - z'|$, one can represent $\mathcal{F}$ and $\partial_z \mathcal{F}$ in the following symmetric form

$$\mathcal{F} = \int_0^{\tau-\tau'} d\varsigma R_0(\varsigma, \tau' - \tau) \frac{S(z + \varsigma, \tau') + S(z - \varsigma, \tau')}{2}, \tag{16}$$

$$\begin{aligned} \partial_z \mathcal{F} &= \frac{S(z + (\tau - \tau'), \tau') - S(z - (\tau - \tau'), \tau')}{2} \\ &\quad - k \int_0^{\tau-\tau'} d\varsigma \varsigma R_1(\varsigma, \tau' - \tau) \frac{S(z + \varsigma, \tau') - S(z - \varsigma, \tau')}{2}. \end{aligned} \tag{17}$$

Thus (13) and (15) yield

$$\Psi(z,\tau)=\int_0^{\tau}d\tau'\int_0^{\tau-\tau'}d\varsigma\,R_0\left(\varsigma,\tau'-\tau\right)\mathrm{Sym}\left[S\right]\left(z,\varsigma,\tau'\right) \tag{18}$$

$$\partial_z\Psi(z,\tau)=\int_0^{\tau}d\tau'\left\{\mathrm{Asym}\left[S\right]\left(z,\tau-\tau',\tau'\right)-k\int_0^{\tau-\tau'}d\varsigma\,\varsigma R_1\left(\varsigma,\tau'-\tau\right)\mathrm{Asym}\left[S\right]\left(z,\varsigma,\tau'\right)\right\}, \tag{19}$$

where

$$\begin{matrix}\mathrm{Sym}\\ \mathrm{Asym}\end{matrix}\left[S\right](z,\varsigma,\tau)\overset{def}{=}\frac{1}{2}\left[S(z+\varsigma,\tau)\pm S(z-\varsigma,\tau)\right] \tag{20}$$

are the two components of the even/odd decomposition of the source

$$S(z+\varsigma,\tau)=\mathrm{Sym}\left[S\right](z,\varsigma,\tau)+\mathrm{Asym}\left[S\right](z,\varsigma,\tau). \tag{21}$$

Now we can state the following:

(i) If for $z=z_0,\forall\varsigma,\tau$ the source exhibits the property

$$S(z_0+\varsigma,\tau)=-S(z_0-\varsigma,\tau) \tag{22}$$

then

$$\Psi(z_0+\varsigma,\tau)=-\Psi(z_0-\varsigma,\tau)\quad\text{and}\quad\Psi|_{z=z_0}=0. \tag{23}$$

(ii) If for $z=z_0,\forall\varsigma,\tau$ the source exhibits the property

$$S(z_0+\varsigma,\tau)=S(z_0-\varsigma,\tau) \tag{24}$$

then

$$\Psi(z_0+\varsigma,\tau)=\Psi(z_0-\varsigma,\tau)\quad\text{and}\quad\partial_z\Psi|_{z=z_0}=0. \tag{25}$$

Using formula (16) one can check by direct calculations that

$$\mathcal{F}\left(\tau',z+\varsigma,\tau\right)=\begin{cases}-\mathcal{F}\left(\tau',z-\varsigma,\tau\right) & \text{case (i)}\\ \mathcal{F}\left(\tau',z-\varsigma,\tau\right) & \text{case (ii)}\end{cases} \tag{26}$$

which, in view of (13), proves the first equations in (23) and (25). In case (i) $\mathrm{Sym}\left[S\right]\equiv 0$ while in case (ii) $\mathrm{Asym}\left[S\right]\equiv 0$, so the second equations in (23) and (25) follow from formulas (18) and (19).

3.2. *Semi-infinite configurations with boundary condition at $z=0$*

Many practically important models (e.g., wave propagation along a semi-infinite waveguide) involve the problem of the previous section defined for a semi-infinite elliptic cylinder, $0<z<\infty$ and an additional homogeneous boundary condition, Dirichlet

$$\Psi(u,v,z,\tau)|_{z=0}=0\Rightarrow\Psi_{mn}^{(e,o)}(z,\tau)\big|_{z=0}=0,\quad\forall m,n \tag{27}$$

or Neumann (normal derivative $\partial_n=-\partial_z$)

$$\partial_z\Psi(u,v,z,\tau)|_{z=0}=0\Rightarrow\partial_z\Psi_{mn}^{(e,o)}(z,\tau)\big|_{z=0}=0,\quad\forall m,n. \tag{28}$$

Here formula (13) yields different solutions of inhomogeneous KGE (6) for different continuations of the source $S_{mn}^{(e,o)}$ to the region $-\infty<z<0$. Problems of type (27) or (28) may be solved using an approach similar to the method of mirror charges: the odd continuation of the source term for $-\infty<z<0$

$$S(u,v,z,\tau)=-S(u,v,-z,\tau)\Rightarrow S_{mn}^{(e,o)}(z,\tau)=-S_{mn}^{(e,o)}(-z,\tau) \tag{29}$$

leads to a particular case of (22), (23) for $z_0=0$, satisfying the Dirichlet boundary condition (27), while the even continuation

$$S(u,v,z,\tau)=S(u,v,-z,\tau)\Rightarrow S_{mn}^{(e,o)}(z,\tau)=S_{mn}^{(e,o)}(-z,\tau), \tag{30}$$

leads to a particular case of (24), (25) for $z_0=0$, thus satisfying the Neumann boundary condition (28). Note that for the initially continuous function S defined so that

$$S|_{z=0}\neq 0\Rightarrow S_{mn}^{(e,o)}\big|_{z=0}\neq 0 \tag{31}$$

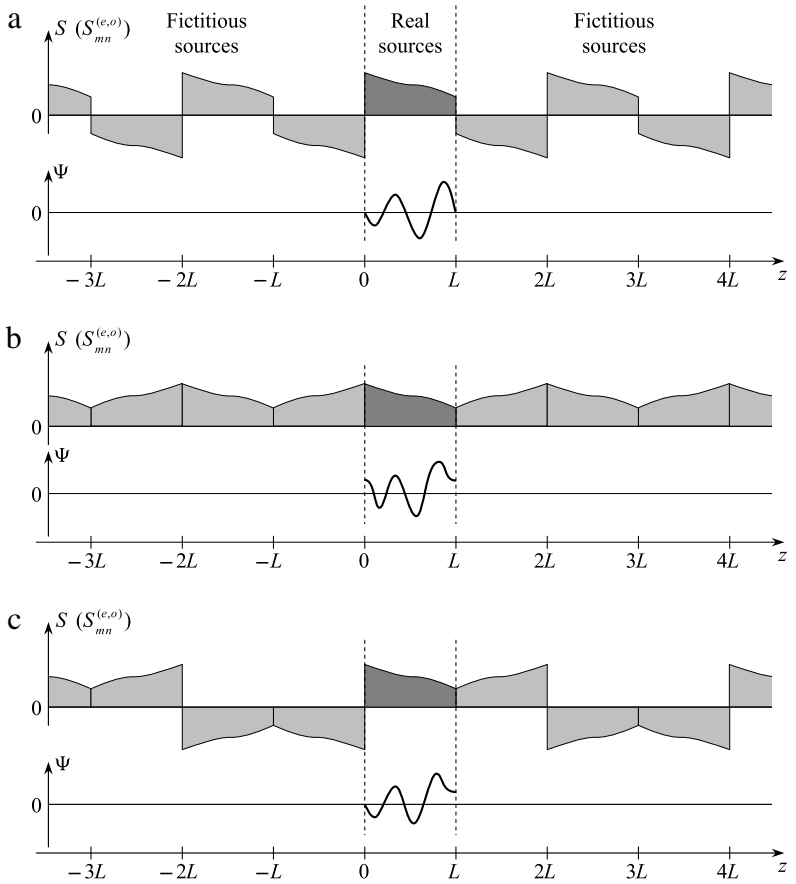

Fig. 3. A scheme of continuation of the source (modal source) $S(S_{m,n}^{(e,o)})$ beyond $0 < z < L$ for the homogeneous Dirichlet (a), Neumann (b), and mixed (c) boundary conditions.

the odd continuation (29) results in the source discontinuity of the first kind at the point $z = 0$ while, as follows from formulas (18), (19) for $z = 0$, $\Psi_{mn}^{(e,o)}$ is continuous at this point with the limiting behavior

$$\Psi_{mn}^{(e,o)}(z,\tau) = \int_0^\tau d\tau' \left[\frac{S_{mn}^{(e,o)}(\tau-\tau',\tau')}{k_{mn}^{(e,o)}} - \int_0^{\tau-\tau'} d\varsigma\, \varsigma \frac{J_1\left(k_{mn}^{(e,o)}\sqrt{(\tau'-\tau)^2-\varsigma^2}\right)}{\sqrt{(\tau'-\tau)^2-\varsigma^2}} S_{mn}^{(e,o)}(\varsigma,\tau') \right] k_{mn}^{(e,o)} z + O\left(\left(k_{mn}^{(e,o)} z\right)^2\right).$$

3.3. Finite-length configurations with boundary conditions at $z = 0, L$

Other practical models (e.g., waves in a cavity) involve the problem defined for the segment $0 < z < L$ with two boundary conditions at $z = 0, L$. In the case of the Dirichlet conditions

$$\Psi(u,v,z,\tau)|_{z=0,L} = 0, \tag{32}$$

we can find the modal solution using formula (13) via the odd continuation of the source

$$S(u,v,z,\tau) = -S(u,v,-z,\tau) \Rightarrow S_{mn}^{(e,o)}(z,\tau) = -S_{mn}^{(e,o)}(-z,\tau) \tag{33}$$

for $-L < z < 0$ and the periodic continuation for $|z| > L$

$$S(u,v,z+2\kappa L,\tau) = S(u,v,z,\tau) \Rightarrow S_{mn}^{(e,o)}(z+2\kappa L,\tau) = S_{mn}^{(e,o)}(z,\tau), \quad \kappa = 0, \pm 1, \pm 2, \ldots. \tag{34}$$

As seen from Fig. 3(a), this leads to $S_{mn}^{(e,o)}(\varsigma,\tau) = -S_{mn}^{(e,o)}(-\varsigma,\tau)$ and $S_{mn}^{(e,o)}(L+\varsigma,\tau) = -S_{mn}^{(e,o)}(L-\varsigma,\tau)$ in the entire axis, so $S_{mn}^{(e,o)}$ exhibits property (22) for $z_0 = 0, L$ and $\forall m, n$, which results in obeying (23) and, consequently, (32).

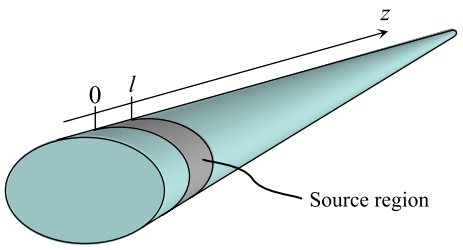

Fig. 4. Waveguide configuration with limited source region.

Using the same approach, it is easy to demonstrate that the Neumann conditions

$$\partial_z \Psi\,(u, v, z, \tau)|_{z=0,L} = 0 \tag{35}$$

are fulfilled provided that the source is evenly continued for $-L < z < 0$

$$S\,(u, v, z, \tau) = S\,(u, v, -z, \tau) \Rightarrow S_{mn}^{(e,o)}\,(z, \tau) = S_{mn}^{(e,o)}\,(-z, \tau) \tag{36}$$

and then subjected to periodic continuation (34). As seen from Fig. 3(b), $S_{mn}^{(e,o)}\,(\varsigma, \tau) = S_{mn}^{(e,o)}\,(-\varsigma, \tau)$ and $S_{mn}^{(e,o)}\,(L + \varsigma, \tau) = S_{mn}^{(e,o)}\,(L - \varsigma, \tau)$. This results in condition (24) being valid for $z_0 = 0, L$ and $\forall m, n$, which brings about (25) and proves (35).

The mixed boundary conditions

$$\Psi\,(u, v, z, \tau)|_{z=0} = 0, \qquad \partial_z \Psi\,(u, v, z, \tau)|_{z=L} = 0 \tag{37}$$

can be satisfied by continuation

$$S\,(u, v, z, \tau) = S\,(u, v, 2L - z, \tau) \Rightarrow S_{mn}^{(e,o)}\,(z, \tau) = S_{mn}^{(e,o)}\,(2L - z, \tau)\,, \tag{38}$$

of the source to the area $L < z < 2L$, followed by the odd continuation to the area $-2L < z < 0$

$$S\,(u, v, z, \tau) = -S\,(u, v, -z, \tau) \Rightarrow S_{mn}^{(e,o)}\,(z, \tau) = -S_{mn}^{(e,o)}\,(-z, \tau) \tag{39}$$

and imposing the $4L$ periodicity

$$S\,(u, v, z + 4\kappa L, \tau) = S\,(u, v, z, \tau) \Rightarrow S_{mn}^{(e,o)}\,(z + 4\kappa L, \tau) = S_{mn}^{(e,o)}\,(z, \tau)\,, \quad \kappa = 0,\ \pm 1,\ \pm 2, \ldots. \tag{40}$$

As illustrated in Fig. 3(c), this continuation corresponds to the $4L$-periodic source for which $S_{mn}^{(e,o)}\,(\varsigma, \tau) = -S_{mn}^{(e,o)}\,(-\varsigma, \tau)$ and $S_{mn}^{(e,o)}\,(L + \varsigma, \tau) = S_{mn}^{(e,o)}\,(L - \varsigma, \tau)$, providing fulfillment of boundary conditions (37).

In a way intuitive conclusions about evenness or oddness of the discussed source continuations with respect to ς based on the schematic plots of Fig. 3 can be strictly proved using the Fourier expansions (whose truncated versions may, in some situations, serve as an approximation of real source distributions), see Appendix B.

4. Finite-length, finite-duration source

Let us consider a source $S\,(u, v, z, \tau)$ limited in the longitudinal direction by the condition $0 < z < l$ (Fig. 4) that, being turned on at the moment $\tau = 0$, acts during a finite time T. Such a source can be explicitly described by the expression

$$S\,(u, v, z, \tau) = h\,(z)\,h\,(l - z)\,h\,(\tau)\,h\,(T - \tau)\,s\,(u, v, z, \tau)\,, \tag{41}$$

where $h\,(z) = \begin{cases} 0 & z < 0 \\ 1 & z > 0 \end{cases}$ is a unit step function and $s\,(u, v, z, \tau)$ is, as previously, some given function.

This leads to the modal representation

$$S_{mn}^{(e,o)}\,(z, \tau) = h\,(z)\,h\,(l - z)\,h\,(\tau)\,h\,(T - \tau)\,s_{mn}^{(e,o)}\,(z, \tau)\,. \tag{42}$$

Formula (13) for the modal amplitudes becomes

$$\Psi_{mn}^{(e,o)}\,(z, \tau) = \frac{1}{2} \iint_{\Omega_{lT}} dz' d\tau' J_0\left(k_{mn}^{(e,o)} \sqrt{(\tau' - \tau)^2 - (z' - z)^2}\right) s_{mn}^{(e,o)}\left(z', \tau'\right), \tag{43}$$

where the shape of the integration area Ω_{lT} shall take into account the boundedness of the support of $S_{mn}^{(e,o)}\,(z, \tau)$. In the following, the Riemann function $J_0\left(k_{mn}^{(e,o)} \sqrt{(\tau' - \tau)^2 - (z' - z)^2}\right)$ is denoted as $R\left(z', \tau'; z, \tau\right)$ and the indices o, e, m and n are dropped.

The sequence of explicit solutions has a number of distinct forms, depending on the interrelations between l, T, z, and τ. They can be derived with the help of a strictly formalized procedure using z', τ' plane diagrams similar to that of Fig. 2.

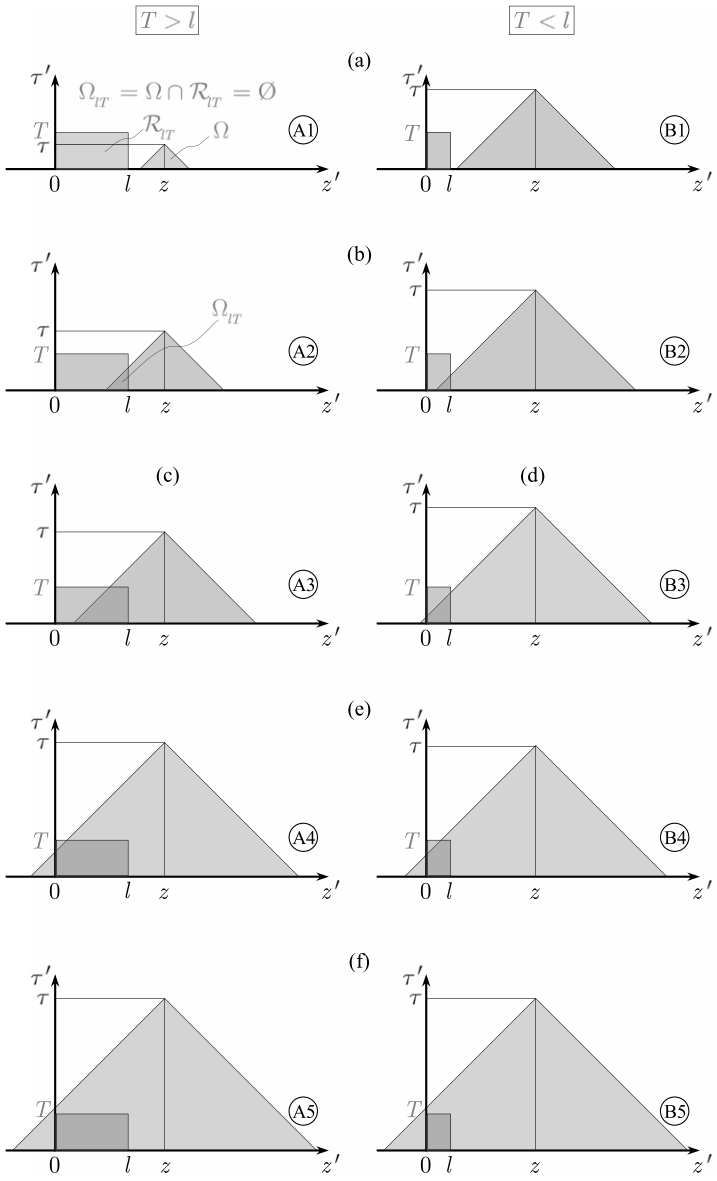

Fig. 5. Integration areas Ω_{lT} for the case of finite-length, finite-duration source (41).

The simplicity of this procedure makes it worthwhile to discuss only the case $z > l$; the results for other ranges of z can be derived straightforwardly within the same conceptual framework.

For $z > l$, the *short-duration pulse* condition $T < l$ partitions the explicit formulas into two sets. Let us suppose that this condition holds and fix the observation point position, $z' = z$, subsequently increasing the observation time from the initial value $\tau = 0$. Then

$$0 < z - l < z - l + T < z < z + T \tag{44}$$

and the following cases can be distinguished:

A1: $0 < \tau < z - l$. As seen from Fig. 5(a), the intersection of the integration area Ω with the domain of source support $\mathcal{R}_{lT} = \{0 \le z' \le l,\ 0 \le \tau' \le T\}$ is empty, $\Omega_{lT} = \Omega \cap \mathcal{R}_{lT} = \emptyset$, and

$$\Psi(z, \tau) = 0. \tag{45}$$

A2: $z - l < \tau < z - l + T$. The integration area Ω_{lT} is shown in Fig. 5(b) and

$$\Psi(z, \tau) = \frac{1}{2} \int_{z-\tau}^{l} dz' \int_{0}^{\tau-(z-z')} d\tau' R\left(z', \tau'; z, \tau\right) s\left(z', \tau'\right). \tag{46}$$

Table 1
Description of the wavefronts defining the space-time structure of the solutions in cases A1–A5 and B1–B5.

Wave-front	Moment of arrival at $z' = z$	Starting point		Information carried
		τ'	z'	
W1	$z - l$	0	l	Source turned on at the point nearest to $z' = z$
W2	$z - l + T$	T	l	Source turned off at the point nearest to $z' = z$
W3	z	0	0	Source turned on at the point farthest to $z' = z$
W4	$z + T$	T	0	Source turned off at the point farthest to $z' = z$

A3: $z - l + T < \tau < z$. The integration area Ω_{lT} is shown in Fig. 5(c) and

$$\Psi(z,\tau) = \frac{1}{2}\left(\int_{z-\tau}^{z-\tau+T} dz' \int_0^{\tau-(z-z')} d\tau' + \int_{z-\tau+T}^{l} dz' \int_0^{T} d\tau'\right) R\left(z',\tau';z,\tau\right) s\left(z',\tau'\right). \tag{47}$$

A4: $z < \tau < z + T$. The integration area Ω_{lT} is shown in Fig. 5(e) and

$$\Psi(z,\tau) = \frac{1}{2}\left(\int_{0}^{z-\tau+T} dz' \int_0^{\tau-(z-z')} d\tau' + \int_{z-\tau+T}^{l} dz' \int_0^{T} d\tau'\right) R\left(z',\tau';z,\tau\right) s\left(z',\tau'\right). \tag{48}$$

A5: $z + T < \tau < \infty$. The integration area $\Omega_{lT} = \mathcal{R}_{lT}$, see Fig. 5(f),

$$\Psi(z,\tau) = \frac{1}{2}\int_0^{l} dz' \int_0^{T} d\tau' R\left(z',\tau';z,\tau\right) s\left(z',\tau'\right). \tag{49}$$

In the opposite situation of the *long-duration pulse* $T > l$ we have

$$0 < z - l < z < z - l + T < z + T \tag{50}$$

and the sequence of cases illustrated in the left side of Fig. 5:

B1: $0 < \tau < z - l$. As seen from Fig. 5(a), the case is identical to case A1 and

$$\Psi(z,\tau) = 0. \tag{51}$$

B2: $z - l < \tau < z$. Apart from the range of variation of τ, the case is identical to case A2, Ω_{lT} is shown in Fig. 5(b), and $\Psi(z,\tau)$ is given by Eq. (46).

B3: $z < \tau < z - l + T$. The case has no analogue in the previous sequence, Ω_{lT} is shown in Fig. 5(d), and

$$\Psi(z,\tau) = \frac{1}{2}\int_0^{l} dz' \int_0^{\tau-(z-z')} d\tau' R\left(z',\tau';z,\tau\right) s\left(z',\tau'\right). \tag{52}$$

B4: $z - l + T < \tau < z + T$. Again, apart from the range of variation of τ, the case is identical to its counterpart A4, see Fig. 5(e), and $\Psi(z,\tau)$ is given by Eq. (48).

B5: $z + T < \tau < \infty$. The case is identical to case A5, $\Psi(z,\tau)$ is given by Eq. (49).

Requiring no causality condition (like retarded nature of the argument, wave propagation in a fixed direction, etc.), the description of waves with the help of the Riemann–Volterra method yields solutions whose space-time structure readily admits interpretation in terms of causal propagation of information: the limiting values of τ defining cases A1–A5 and B1–B5 correspond to the moments of arrival, at the point $z' = z$, the wavefronts described in Table 1, propagating along the z direction with the speed c. The short-duration pulse condition $T < l$ imposes the arrival of the wavefronts in the sequence W1–W4, while in the opposite case $T > l$ they arrive in the sequence W1–W4. This short analysis demonstrates that cases like A1–A4 (B1–B4) arise due to inherent properties of the imposed space-time constraints rather than due to some mathematical trickery.

An example of the modal amplitudes $\Psi_{01}^{(e)}$, $\Psi_{11}^{(e)}$, and $\Psi_{11}^{(o)}$ calculated for a long-duration pulse is given in Fig. 6. Although the source-pulse duration is finite, the waveguide, rather than free-space, propagation regime disperse the wave modes over the entire range $z - l < \tau < \infty$ (see [2,3], especially the discussion on results presented in Figs. 10 and 11 of Ref. [3]).

5. Finite-length, finite-duration source pulse traveling at constant speed

The general form of limited source (41) discussed in the previous section admits, in particular, simultaneous wave excitation in the entire volume of the elliptic cylinder $0 < z < l, 0 \le u < u_0$. Many practical problems of acoustics and, especially, electrodynamics, involve more restrictive models of a traveling pulsed source propagating with finite speed. In this section the application of the developed ansatz is illustrated for the case of a pulsed source generated at the cross-section $z = 0$ from $\tau = 0$ to T, and traveling at a constant speed βc along the z axis till $z = l$. To demonstrate the technique

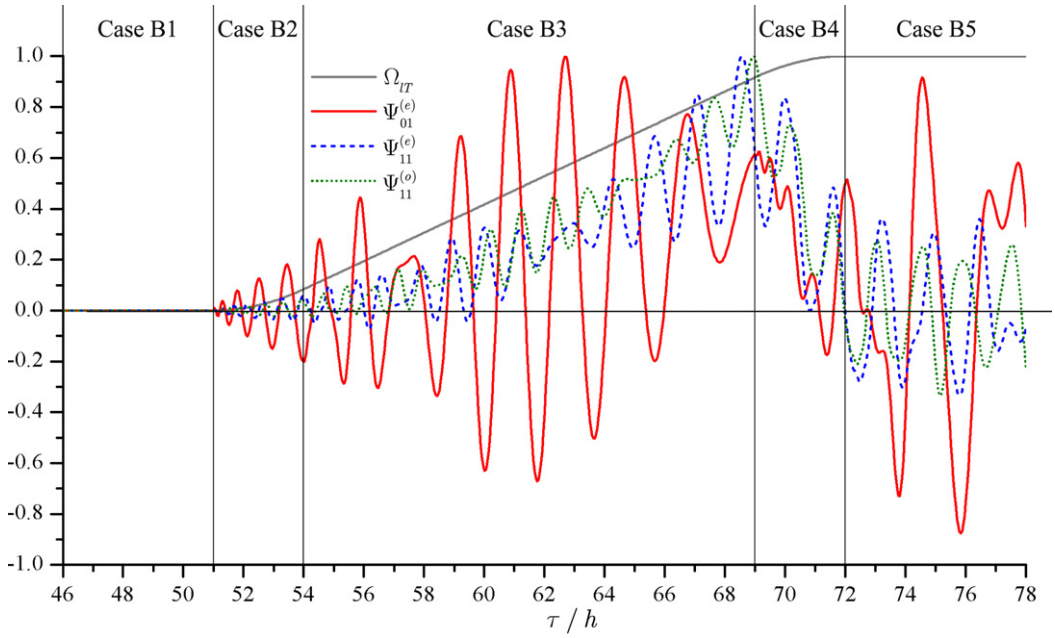

Fig. 6. Dependence of the unity-normalized integration area Ω_{IT} and the first three elliptic modes $\psi_{01}^{(e)}$, $\psi_{11}^{(e)}$, $\psi_{11}^{(o)}$ on the dimensionless time τ/h for cases B1–B5. The observation point is fixed at $z/h = 54$ while $T/h = 18$ and $l/h = 3$ (long-duration pulse).

developed in Section 3.2, let us suppose that the problem is posed for a semi-infinite waveguide, $0 < z < \infty$, and involves Dirichlet boundary condition (27). In this situation the source can be represented in the explicit form

$$\begin{aligned} S(u, v, z, \tau) &= h(l - z)\, h(\tau)\, h(\beta\tau - z)\, h(z - \beta(\tau - T))\, s(u, v, z, \tau) \\ &= h(l - z)\, h(\beta\tau - z)\, h(z - \beta\tau + \beta T)\, s(u, v, z, \tau), \quad z > 0, \end{aligned} \tag{53}$$

where $s(u, v, z, \tau)$ is a given function. Correspondingly,

$$S_{mn}^{(e,o)}(z, \tau) = h(l - z)\, h(\beta\tau - z)\, h(z - \beta\tau + \beta T)\, s_{mn}^{(e,o)}(z, \tau), \tag{54}$$

where $s_{mn}^{(e,o)}(z, \tau)$ is a known function derived from $s(u, v, z, \tau)$ using Eqs. (A.1) and (A.2). The odd continuation of the source required for satisfaction of the boundary condition is

$$S_{mn}^{(e,o)}(z, \tau) = \begin{cases} h(l - z)\, h(\beta\tau - z)\, h(\beta(T - \tau) + z)\, s_{mn}^{(e,o)}(z, \tau) & \text{for } z > 0 \\ h(l + z)\, h(\beta\tau + z)\, h(\beta(T - \tau) - z)\, s_{mn}^{(e,o)}(z, \tau) & \text{for } z < 0, \end{cases} \tag{55}$$

where, to satisfy (33), the function $s_{mn}^{(e,o)}(z, \tau)$ is defined for $-\infty < z < 0$ according to the rule

$$s_{mn}^{(e,o)}(z, \tau) = -s_{mn}^{(e,o)}(-z, \tau) \tag{56}$$

within the V-shaped domain of the source support $\mathcal{V}_{IT} = \{-l \le z \le l,\ |z|/\beta \le \tau \le |z|/\beta + T\}$ shown in Fig. 7.

We will consider a particular case

$$\beta < 1, \qquad \frac{1 - \beta}{\beta} l < T < 2l \Rightarrow T < \frac{1 + \beta}{\beta} l, \qquad T + \frac{1 - \beta}{\beta} l < \frac{1 + \beta}{\beta} l, \tag{57}$$

and, for the purpose of more comprehensive illustration, fix the observation time τ (instead of fixing the observation location, as is done in the previous section) so that

$$\tau > T + \frac{1 + \beta}{\beta} l. \tag{58}$$

In this situation

$$0 < \tau - \frac{1 + \beta}{\beta} l - T < \tau - \frac{1 + \beta}{\beta} l < \tau - \frac{1 - \beta}{\beta} l - T < \tau - T < \tau - \frac{1 - \beta}{\beta} l < \tau, \tag{59}$$

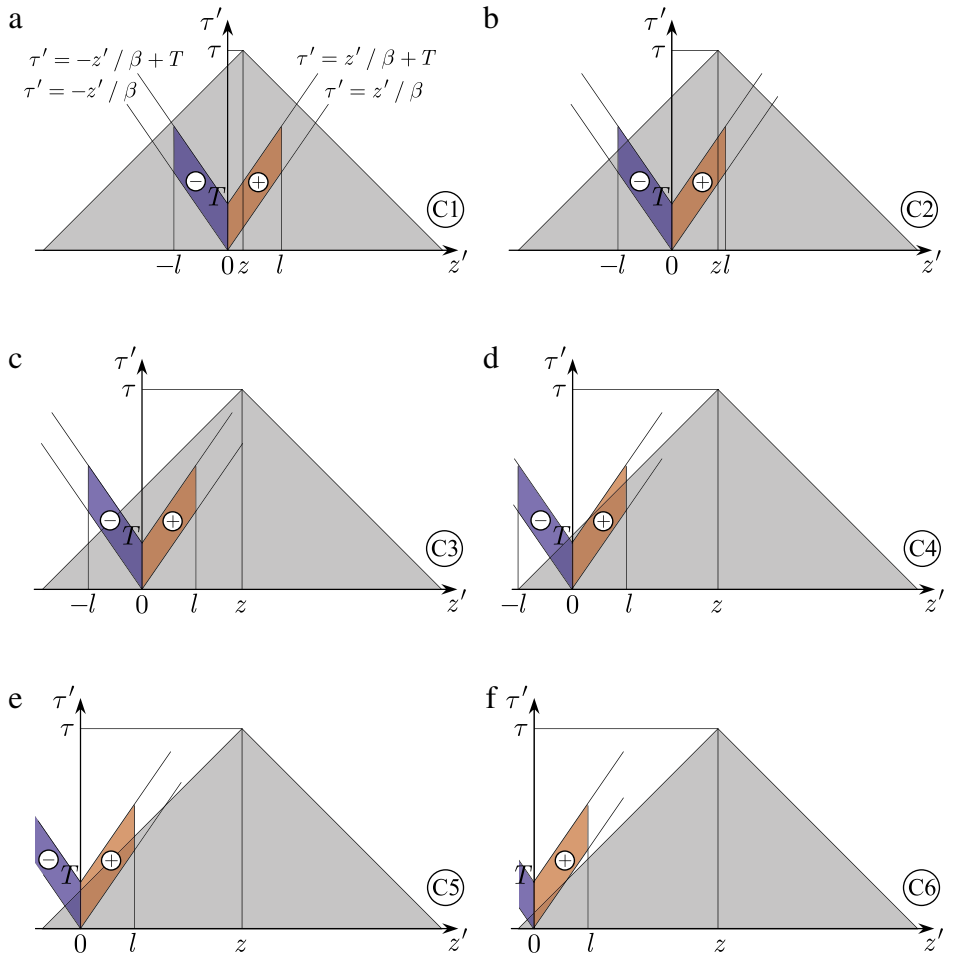

Fig. 7. Integration areas Ω_{IT} for the case of finite-length, finite-duration source pulse traveling at constant speed along a semi-infinite waveguide.

giving rise to the following cases illustrated in Fig. 7:

C1: $0 < z < \tau - \frac{1+\beta}{\beta} l - T$. As seen from Fig. 7(a), in this initial case the integration area Ω covers entirely the domain of source support $\mathcal{V}_{IT}$, so $\Omega_{IT} = \Omega \cap \mathcal{V}_{IT} = \mathcal{V}_{IT}$. Reducing, with the help of change of variable $z' \to -z' \ \left(z' < 0\right)$, the integration to the area containing only real (i.e., non-fictitious) source, $z > 0$, one gets

$$\Psi\left(z, \tau\right) = \frac{1}{2} \int_0^l dz' \int_{z'/\beta}^{z'/\beta+T} d\tau' \left[R\left(z', \tau'; z, \tau\right) - R\left(-z', \tau'; z, \tau\right)\right] s\left(z', \tau'\right) \tag{60}$$

(again, the indices o, e, m and n are dropped).

C2: $\tau - \frac{1+\beta}{\beta} l - T < z < \tau - \frac{1+\beta}{\beta} l$. As illustrated in Fig. 7(b), in the segment $-l < z' < 0$ we have two different limits of integration over τ' depending on whether z' less or greater than $-\frac{\beta}{1+\beta}\left(\tau - z - T\right)$. After a change of the integration variable $z'' = -z'$ for $-l < z' < 0$ that, as in the previous case, restricts the integration to the area of real sources, concretization of formula (43) reads

$$\begin{aligned}\Psi\left(z, \tau\right) = {} & \frac{1}{2} \int_0^l dz' \int_{z'/\beta}^{z'/\beta+T} d\tau' R\left(z', \tau'; z, \tau\right) s\left(z', \tau'\right) \\ & - \frac{1}{2} \left[\int_0^{\frac{\beta}{1+\beta}(\tau-z-T)} dz'' \int_{z'/\beta}^{z'/\beta+T} d\tau' + \int_{\frac{\beta}{1+\beta}(\tau-z-T)}^{l} dz'' \int_{z'/\beta}^{-z''-z+\tau} d\tau' \right] \\ & \times R\left(-z'', \tau'; z, \tau\right) s\left(z'', \tau'\right). \end{aligned} \tag{61}$$

C3: $\tau - \frac{1+\beta}{\beta} l < z < \tau - \frac{1-\beta}{\beta} l - T$. In contrast to case C2, in the area of negative z' the integration domain is restricted by the segment $-\frac{\beta}{1+\beta}(\tau - z) < z' < 0$ (see Fig. 7(c)), which yields

$$\Psi(z,\tau) = \frac{1}{2}\int_0^l dz' \int_{z'/\beta}^{z'/\beta+T} d\tau' R(z',\tau';z,\tau)\, s(z',\tau') - \frac{1}{2}\left[\int_0^{\frac{\beta}{1+\beta}(\tau-z-T)} dz'' \int_{z'/\beta}^{z'/\beta+T} d\tau' + \int_{\frac{\beta}{1+\beta}(\tau-z-T)}^{\frac{\beta}{1+\beta}(\tau-z)} dz'' \int_{z'/\beta}^{-z''-z+\tau} d\tau'\right] R(-z'',\tau';z,\tau)\, s(z'',\tau'). \quad (62)$$

C4: $\tau - \frac{1-\beta}{\beta} l - T < z < \tau - T$. As seen from Fig. 7(d), the area Ω starts cutting the right part of the source support, resulting in appearance of two different limits of integration over τ' for $0 < z' < \frac{\beta}{1-\beta}(\tau - z - T)$ and $\frac{\beta}{1-\beta}(\tau - z - T) < z' < l$, which results in

$$\Psi(z,\tau) = \frac{1}{2}\left[\int_0^{\frac{\beta}{1-\beta}(\tau-z-T)} dz' \int_{z'/\beta}^{z'/\beta+T} d\tau' + \int_{\frac{\beta}{1-\beta}(\tau-z-T)}^{l} dz' \int_{z'/\beta}^{z'-z+\tau} d\tau'\right] R(z',\tau';z,\tau)\, s(z',\tau') - \frac{1}{2}\left[\int_0^{\frac{\beta}{1+\beta}(\tau-z-T)} dz'' \int_{z'/\beta}^{z'/\beta+T} d\tau' + \int_{\frac{\beta}{1+\beta}(\tau-z-T)}^{\frac{\beta}{1+\beta}(\tau-z)} dz'' \int_{z'/\beta}^{-z''-z+\tau} d\tau'\right] \times R(-z'',\tau';z,\tau)\, s(z'',\tau'). \quad (63)$$

C5: $\tau - T < z < \tau - \frac{1-\beta}{\beta} l$. The intersection of Ω and $\mathcal{V}_{IT}$ result in the unique upper limit of integration over $\tau', z' - z + \tau$ (taking the form $-z'' - z + \tau$ for negative z'), see Fig. 7(e), leading to

$$\Psi(z,\tau) = \frac{1}{2}\int_0^l dz' \int_{z'/\beta}^{z'-z+\tau} d\tau' R(z',\tau';z,\tau)\, s(z',\tau') - \frac{1}{2}\int_0^{\frac{\beta}{1+\beta}(\tau-z)} dz'' \int_{z''/\beta}^{-z''-z+\tau} d\tau' R(-z'',\tau';z,\tau)\, s(z'',\tau'). \quad (64)$$

C6: $\tau - \frac{1-\beta}{\beta} l < z < \tau$. Here the area of positive z' the integration domain is restricted by the segment $\frac{\beta}{1-\beta}(\tau - z) < z' < l$ as shown in Fig. 7(e), which yields

$$\Psi(z,\tau) = \frac{1}{2}\int_0^{\frac{\beta}{1-\beta}(\tau-z)} dz' \int_{z'/\beta}^{z'-z+\tau} d\tau' R(z',\tau';z,\tau)\, s(z',\tau') - \frac{1}{2}\int_0^{\frac{\beta}{1+\beta}(\tau-z)} dz'' \int_{z'/\beta}^{-z''-z+\tau} d\tau' R(-z'',\tau';z,\tau)\, s(z'',\tau'). \quad (65)$$

C7: $\tau < z < \infty$. In this last case $\Omega_{IT} = \Omega \cap \mathcal{V}_{IT} = \emptyset$ and $\Psi(z,\tau) = 0$.

As in the situation of the previous section, one can straightforwardly describe the subdivision of the integration procedure into cases C1–C7 in terms of propagation of information. For example, the segment of z' corresponding to case C6 is delimited by the wavefront from the source pulse initially turned on at $\tau' = 0, z' = 0$ (for $\tau' = \tau$, positioned at $z' = \tau$) and the wavefront from the source turned off at the end of its trajectory $\tau' = l/\beta, z' = l$ (for $\tau' = \tau$, positioned at $z' = l + \tau - l/\beta$). Here an important additional phenomenon is the reflection of counter-propagating wavefronts on the boundary $z = 0$.

Fig. 8 illustrates the dependence of the normalized integration area Ω_{IT} on the dimensionless longitudinal coordinate z/h for cases C1–C7 plotted together with snapshots of the first three unity-normalized elliptic modes $\Psi_{01}^{(e)}$, $\Psi_{11}^{(e)}$, and $\Psi_{11}^{(o)}$. As these modes are generated by a more complex transient source than those discussed in Refs. [2–5], they exhibit far more complicated structure.

6. Conclusions

In this article we first have shown how the well-known classical expansion in terms of the Mathieu functions, describing the steady-state vibrational modes of a stretch membrane having an elliptical boundary, can be transformed to transient modal solutions of the inhomogeneous wave equations related to contemporary topical problems, in particular, the problems of propagation of ultra-short (ultra wideband) pulses within elliptic waveguides. Notably, the completeness of the Mathieu sine and cosine modes enables one to construct a general modal solution for the case of arbitrary initial conditions imposed upon Ψ and $\partial_\tau \Psi$. A part of the problem-solving procedure is the introduction of the specific Klein–Gordon equation ansatz based on the Riemann–Volterra method, which has significant independent merit and constitutes the

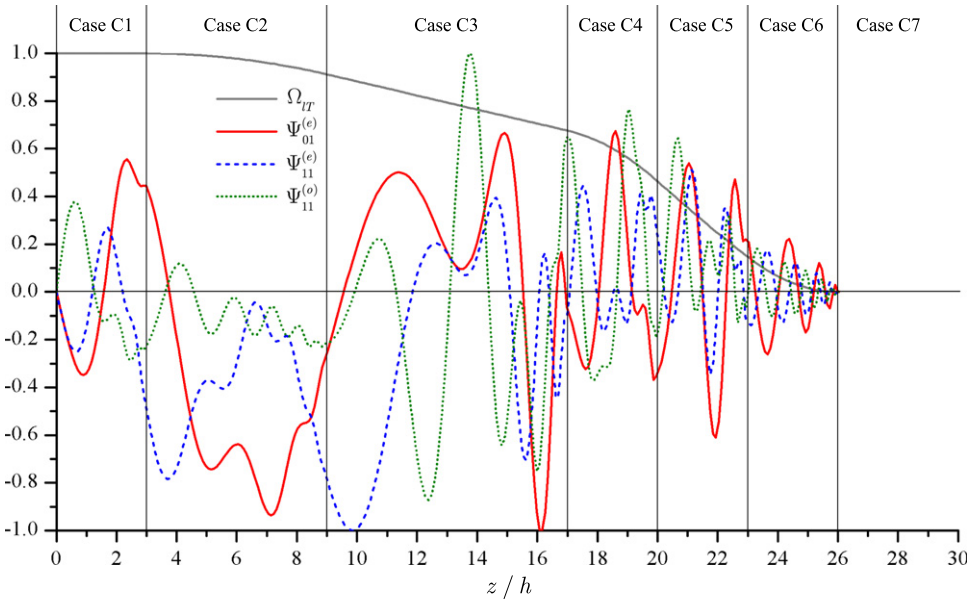

Fig. 8. Dependence of the integration area Ω_{IT} (normalized to 2lT) on the dimensionless longitudinal coordinate z/h for cases C1–C7 plotted together with snapshots of the first three unity-normalized elliptic modes $\psi_{01}^{(e)}$, $\psi^{(e)}11$, and $\psi_{11}^{(o)}$. The dimensionless time τ/h is fixed at 26 while $\beta = 0.7$, $l/h = 7$, and $T/h = 6$.

second objective of the article. Application of this ansatz is not restricted to the elliptic cross-section geometry; it can be equally applied to KGEs resulted from many modern analytical approaches to solving the wave and Maxwell's equations without resorting to the frequency Fourier analysis [1–7].

Focusing on these principal goals, the article omits:

(i) Specific issues related to the vector nature of the electromagnetic waves, reduction of Maxwell's equations to the set of scalar wave equations, and reduction of the specific boundary conditions for the field components to the homogeneous boundary conditions imposed upon scalar wavefunctions. For the case of elliptic geometry, detailed treatment of the subject can be found in [15, Chapter XIX] and [14,20–23], while Refs. [2–5] analyze more powerful and universal methods, suitable for general-type cylindrical waveguides, comprising simultaneous scalarization of Maxwell's equations and separation of the transverse variables.

(ii) Discussion of the transverse structure of the constructed transient modes. Such a structure, corresponding to the classical Mathieu modes, is widely considered in the literature (see, for example, illustrations in [24] and a plot package [25]).

(iii) Techniques for computation of the resulting integral solutions. Although the explicit consideration of the actual, essentially bounded, integration domains significantly alleviates the computational burden (cf. the solution obtained in [2, Section 5.2], and [3, Appendix C]), calculation of the final integrals requires special consideration in the domains of rapid oscillation of the Riemann function. Such a necessity, however, cannot be regarded as a serious drawback of the method, as the easy-to-estimate asymptotic behavior of $J_0(\cdot)$ makes possible application of efficient analytical [26] and numerical techniques [27].

Extension of the method to other models is the most straightforward for the circular cylindrical coordinate system. The Klein–Gordon problems resulting from application of the transverse–longitudinal decomposition [2,5] and expansions by eigenvalues [3] can also be solved using the Riemann–Volterra method. The space-time domain approach to the problems of wave propagation in the spherical coordinate system—for example, the transient-multipole expansion—leads to the Euler–Poisson–Darboux, rather than to the Klein–Gordon, equation. The fact that this equation also has a known Riemann function enables the procedure of Section 2 to be easily adapted to the case. Finally, Olevskii's theorem [28] opens the prospect of construction of the Riemann functions to more complicated PDEs, extending the method to description of such phenomena as wave propagation in dispersive media [9].

In the developed method, at increasing the spatial or temporal coordinate of the observation point, the integration domain changes its shape, giving rise to case formulas. As discussed in Sections 4 and 5, the case structure is not a kind of mathematical trickery inherent to the particular realization of the Riemann–Volterra solvers: generation of a pulsed transient current is accompanied by a series of events, and different cases correspond to different sequences in which the information about these events comes at the observation point. On the other hand, popular time-domain methods based on Green functions yield apparently different results with initially infinite, rather than triangle, domains of integration. Without going into a detailed discussion, let us point up the similarity between the two approaches. Here the key point is

formula 3.876.1 of [29]

$$\int_0^\infty dx \frac{\sin\left(q\sqrt{x^2+a^2}\right)}{\sqrt{x^2+a^2}}\cos(bx) = \frac{\pi}{2}J_0\left(a\sqrt{q^2-b^2}\right)h(q-b), \tag{66}$$

that in the simplest case of an infinite source pulse launched at $\tau = 0$ (discussed, for example, by Geyi [3]) yields for the Green function technique the same integrand as the Riemann–Volterra method and an X-shaped integration domain $z - \left|\tau' - \tau\right| < z' < z + \left|\tau' - \tau\right|$ that, together with another condition implied on the source support, $0 < \tau' < \tau$ due to causality, brought us to the same triangle domain of integration as the Riemann–Volterra procedure of Section 2 (Fig. 2) with the kernel

$$\begin{aligned} G_n(z,\tau;z',\tau') &= \frac{c}{\pi}\int_0^\infty dp\, \frac{\sin\left((\tau-\tau')\sqrt{p^2+k_{mn}^2}\right)}{\sqrt{p^2+k_{mn}^2}}\cos\left(p(z-z')\right) \\ &= \frac{c}{2}J_0\left(k_{mn}\sqrt{(\tau'-\tau)^2-(z'-z)^2}\right)h\left(\tau-\tau'-\left|z-z'\right|\right), \end{aligned} \tag{67}$$

see Ref. [3, Eq. (16)].

As spatiotemporal description of essentially nonsinusoidal ultrashort electromagnetic pulses gains increasing importance for localized wave generation, anti-stealth radar applications, electronic warfare and radio-frequency weaponization [30], the author believe that the method introduced in the article may also find several practicable applications in study of signal and precursor propagation in media [31,32], optimization of cavities, waveguides and UWB emitters [33] as well as in the assessment of the vulnerability of microwave and electronic systems to voltage and current surges [4].

Appendix A. Expansion in terms of Mathieu modes

For arbitrary integrable function $\zeta(u,v)$, the coefficients of the expansion of type (4) can be obtained using the orthogonality properties of the Mathieu modes as discussed in Section 16.15 of Ref. [15]:

$$\zeta_{mn}^{(e)} = \frac{\int_0^{u_0} du \int_0^{2\pi} dv\ \zeta(u,v)\,\mathrm{Ce}_m\left(u,q_{mn}^{(e)}\right)\mathrm{ce}_m\left(v,q_{mn}^{(e)}\right)(\cosh 2u - \cos 2v)}{\pi\int_0^{u_0} du \mathrm{Ce}_m^2\left(u,q_{mn}^{(e)}\right)\left(\cosh 2u - \Theta_{mn}^{(e)}\right)}, \tag{A.1}$$

$$\zeta_{mn}^{(o)} = \frac{\int_0^{u_0} du \int_0^{2\pi} dv\ \zeta(u,v)\,\mathrm{Se}_m\left(u,q_{mn}^{(o)}\right)\mathrm{se}_m\left(v,q_{mn}^{(o)}\right)(\cosh 2u - \cos 2v)}{\pi\int_0^{u_0} du \mathrm{Se}_m^2\left(u,q_{mn}^{(o)}\right)\left(\cosh 2u - \Theta_{mn}^{(o)}\right)}, \tag{A.2}$$

where

$$\begin{pmatrix}\Theta_{mn}^{(e)}\\ \Theta_{mn}^{(o)}\end{pmatrix} = \frac{1}{\pi}\int_0^{2\pi} dv \begin{pmatrix}\mathrm{ce}_m^2\left(v,q_{mn}^{(e)}\right)\\ \mathrm{se}_m^2\left(v,q_{mn}^{(o)}\right)\end{pmatrix}\cos 2v. \tag{A.3}$$

Appendix B. Proof of oddness or evenness of the source continuations for finite-length configurations

(a) *Dirichlet boundary conditions* (32). The $2L$-periodic definition of the source (33), (34) can be expanded into the Fourier series (in order not to clutter the formulas, the dependence on u, v, and τ is dropped)

$$S(z) = \sum_{j=1}^\infty S_j \sin\left(j\pi\frac{z}{L}\right), \qquad S_j = \frac{1}{L}\int_{-L}^{L} S(z)\sin\left(j\pi\frac{z}{L}\right)dz = \frac{2}{L}\int_0^L S(z)\sin\left(j\pi\frac{z}{L}\right)dz, \tag{B.1}$$

all cosine coefficients being zero due to (33). From this follows $S(\varsigma) = -S(-\varsigma)$, $-\infty < \varsigma < \infty$, that is, property (22) for $z_0 = 0$. The source representation as a function of $L+\varsigma$ takes the form providing the same property for $z_0 = L$:

$$S(L+\varsigma) = \sum_{j=1}^\infty S_j \sin\left(j\pi\frac{L+\varsigma}{L}\right) = \sum_{j=1}^\infty (-1)^j S_j \sin\left(j\pi\frac{\varsigma}{L}\right) = -S(L-\varsigma). \tag{B.2}$$

(b) *Neumann boundary conditions* (35). The analogous Fourier expansion of the $2L$-periodic source (34), (36) is

$$S(z) = \frac{1}{2}S_0 + \sum_{j=1}^\infty S_j \cos\left(j\pi\frac{z}{L}\right), \qquad S_j = \frac{1}{L}\int_{-L}^{L} S(z)\cos\left(j\pi\frac{z}{L}\right)dz = \frac{2}{L}\int_0^L S(z)\cos\left(j\pi\frac{z}{L}\right)dz, \tag{B.3}$$

all sine coefficients being zero in view of (36), so $S(\varsigma) = S(-\varsigma)$. The source representation as a function of $L+\varsigma$ is

$$S(L+\varsigma) = \frac{1}{2}S_0 + \sum_{j=1}^{\infty} S_j \cos\left(j\pi\frac{L+\varsigma}{L}\right) = \frac{1}{2}S_0 + \sum_{j=1}^{\infty}(-1)^j S_j \cos\left(j\pi\frac{\varsigma}{L}\right) = S(L-\varsigma). \tag{B.4}$$

Thus the source possesses property (24) for both $z_0 = 0$ and $z_0 = L$.

(c) *Mixed boundary conditions* (37). Here $4L$-periodic odd source (38)–(40) can be represented via the Fourier series

$$S(z) = \sum_{j=1}^{\infty} S_j \sin\left(j\pi\frac{z}{2L}\right), \tag{B.5}$$

where

$$\begin{aligned} S_j &= \frac{1}{2L}\int_{-2L}^{2L} S(z)\sin\left(j\pi\frac{z}{2L}\right)dz = \frac{1}{L}\int_0^{2L} S(z)\sin\left(j\pi\frac{z}{2L}\right)dz \\ &= \frac{1}{L}\left[\int_0^{L} S(z)\sin\left(j\pi\frac{z}{2L}\right)dz + \int_L^{2L} S(z)\sin\left(j\pi\frac{z}{2L}\right)dz\right]. \end{aligned} \tag{B.6}$$

Using the continuation rule (38) and the integration variable $\tilde{z} = 2L - z$, the last integral can be rewritten as

$$\begin{aligned} \int_L^{2L} S(2L-z)\sin\left(j\pi\frac{z}{2L}\right)dz &= \int_0^{L} S(\tilde{z})\sin\left(j\pi - j\pi\frac{\tilde{z}}{2L}\right)d\tilde{z} \\ &= (-1)^{j+1}\int_0^{L} S(\tilde{z})\sin\left(j\pi\frac{\tilde{z}}{2L}\right)d\tilde{z}, \end{aligned} \tag{B.7}$$

zeroing the coefficient S_j for any even j. Thus the summation in (B.5) must be carried out over odd indices, reducing the series into

$$S(z) = \sum_{j=1}^{\infty} S_{2j+1}\sin\left((2j+1)\pi\frac{z}{2L}\right), \tag{B.8}$$

which readily provides property (22) for $z_0 = 0$ and, taking the form

$$\begin{aligned} S(L+\varsigma) &= \sum_{j=1}^{\infty} S_{2j+1}\sin\left((2j+1)\pi\frac{L+\varsigma}{2L}\right) \\ &= \sum_{j=1}^{\infty}(-1)^{j+1} S_{2j+1}\cos\left((2j+1)\pi\frac{\varsigma}{2L}\right) = S(L-\varsigma), \end{aligned} \tag{B.9}$$

property (24) for $z_0 = L$.

References

[1] O.A. Tretyakov, Analytical and Numerical Methods in Electromagnetic Wave Theory, Science House Co. Ltd, Tokyo, 1992, Chapter 3.
[2] G. Kristensson, Transient electromagnetic wave propagation in waveguides, J. Electromagnetics Waves and Appl. 9 (1995) 645–671.
[3] W. Geyi, A time-domain theory of waveguide, Prog. Electromagnetics Res. 59 (2006) 267–297.
[4] F. Erden, O.A. Tretyakov, Excitation by a transient signal of the real-valued electromagnetic fields in a cavity, Phys. Rev. E 77 (2008) 056605.
[5] O.A. Tretyakov, O. Akgun, Derivation of Klein–Gordon equation from Maxwell's equations and study of relativistic time-domain waveguide modes, Progress In Electromagnetics Research 105 (2010) 171–191.
[6] L.C. Evans, Partial Differential Equations, 2nd ed. American Mathematical Society, Providence, R.I, 2010, Section 6.5.
[7] W. Miller, Symmetry and Separation of Variables, Addison-Wesley, Boston, MA, 1977.
[8] V.V. Borisov, A.V. Manankova, A.B. Utkin, Spherical harmonic representation of the electromagnetic field produced by a moving pulse of current density, J. Phys. A: Math. Gen. 29 (1996) 4493–4514.
[9] V.V. Borisov, On spherical harmonic representation of transient waves in dispersive media, J. Phys. A: Math. Gen. 36 (2003) 10131–10140.
[10] V.V. Borisov, A.B. Utkin, Transient electromagnetic field produced by a moving pulse of line current, J. Phys. D: Appl. Phys. 28 (1995) 614–622.
[11] V.V. Borisov, Nonsteady-State Fields in Waveguides, Leningrad State University Press, Leningrad, 1991.
[12] A.C. Perdikouris, D.P. Chrissoulidis, E.E. Kriezis, EM-wave propagation through semi-elliptic cylindrical dielectric waveguide on a perfectly conductive planar substrate, IEEE Trans. Microw. Theory Tech. 42 (1994) 891–898.
[13] G.D. Tsogkas, J.A. Roumeliotis, S.P. Savaidis, Cutoff wavelengths of elliptical metallic waveguides, IEEE Trans. Microw. Theory Tech. 57 (2009) 2406–2415.
[14] K. Halterman, S. Feng, P.L. Overfelt, Guided modes of elliptical metamaterial waveguides, Phys. Rev. A 76 (2007) 013834.
[15] N.W. McLachlan, Theory and Applications of Mathieu Functions, Dover, New York, 1964.
[16] S. Goldstein, Mathieu functions, Trans. Cambridge Philos. Soc. 23 (1927) 303–336.
[17] G.A. Korn, T.M. Korn, Mathematical Handbook for Scientists and Engineers: Definitions, Theorems, and Formulas for Reference and Review, Dover Publications, New York, 2000, pp. 309–310.
[18] V.I. Smirnov, A Course Of Higher Mathematics, Vol. 4, Oxford, Pergamon, 1964, Part 2, Section 4.
[19] F.W.J. Olver, D.W. Lozier, R.F. Boisvert, C.W. Clark, NIST Handbook of Mathematical Functions, NIST and Cambridge Univ. Press, Cambridge, 2010.

[20] E.T. Whittaker, On an expression of the electromagnetic field due to electrons by means of two scalar potential functions, Proc. Lond. Math. Soc. 1 (1904) 367–372.
[21] A. Nisbet, Hertzian electromagnetic potentials and associated gauge transformations, Proc. R. Soc. Lond. Ser. A 231 (1955) 250–263.
[22] M.J. Lahart, Use of electromagnetic scalar potentials in boundary value problems, Am. J. Phys. 72 (2004) 83–91.
[23] L.J. Chu, Electromagnetic waves in elliptic hollow pipes of metal, J. Appl. Phys. 9 (1938) 583–591.
[24] J.C. Gutiérrez-Veja, R.M. Rodríguez-Dagnino, M.A. Meneses-Nava, S. Chávez-Cerda, Mathieu functions, a visual approach, Am. J. Phys. 71 (2003) 233–242.
[25] H. Wilson, A. Matlab® package providing animated color plots of the Mathieu modes, http://www.mathworks.se/matlabcentral/fileexchange/6500-vibration-modes-of-an-elliptic-membrane.
[26] J. Kaplunov, V. Voloshin, A.D. Rawlins, Uniform asymptotic behaviour of integrals of Bessel functions with a large parameter in the argument, Quart. J. Mech. Appl. Math. 63 (2010) 57–72.
[27] NAG numerical libraries, http://www.nag.co.uk/numeric/numerical_libraries.asp.
[28] M.N. Olevskii, On the Riemann function for the differential equation $\partial^2 u/\partial x^2 - \partial^2 u/\partial \tau^2 + (p_1(x) + p_2(\tau))\, u = 0$, Dokl. Akad. Nauk SSSR 87 (1952) 337–340.
[29] I.S. Gradshteyn, I.M. Ryzhik, Table of Integrals,Series and Produts, 6th ed. Academic Press, London, 2000.
[30] C. Fowler, J. Entzminger, J. Corum, Assessment of ultra-wideband (UWB) technology, IEEE Aerosp. Electron. Syst. Mag. 5 (1990) 45–49.
[31] J.E. Macías-Díaz, On the controlled propagation of wave signals in a sinusoidally forced two-dimensional continuous Frenkel–Kontorova model, Wave Motion 48 (2011) 13–23.
[32] L. Rapoport, Z. Katzir, M.B. Rubin, Termination of the starting problem of dynamic expansion of a spherical cavity in an infinite elastic-perfectly-plastic medium, Wave Motion 48 (2011) 441–452.
[33] S.N. Ivanov, G.A. Mesyats, V.G. Shpak, Subnanosecond X-ray apparatus with flexible cable radiator probe based on small-size explosive emission vacuum diode, JINST 6 (2011) P0500.

Andrei B. Utkin was born in St. Petersburg in 1959. He received his Honor M.Sc. (1982) and Ph.D. (1986) degrees in Physics and Mathematics from Leningrad (now St. Petersburg) State University, Russia, and equivalence to Ph.D. degree in Physics from Technical University of Lisbon (2007). He is currently investigator in INOV — INESC Inovação (Lisbon, Portugal). His areas of research interest include electromagnetics, lidar, spectrometry, signal processing and pattern recognition.